

Analysis of cosmic ray neutron-induced single-event phenomena

Yasuyuki TUKAMOTO, Yukinobu WATANABE, and Hideki NAKASHIMA

*Department of Advanced Energy Engineering Science, Kyushu University,
Kasuga, Fukuoka 816-8580, Japan*

Corresponding email: watanabe@aees.kyushu-u.ac.jp

We have developed a database of cross sections for the $n+^{28}\text{Si}$ reaction in the energy range between 2 MeV and 3 GeV in order to analyze single-event upset (SEU) phenomena induced by cosmic-ray neutrons in semiconductor memory devices. The data are applied to calculations of SEU cross sections using the Burst Generation Rate (BGR) model including two parameters, critical charge and effective depth. The calculated results are compared with measured SEU cross-sections for energies up to 160 MeV, and the reaction products that provide important effects on SEU are mainly investigated.

1. Introduction

In recent years, much concerns has been paid to cosmic-ray induced soft errors in semiconductor memory devices used on ground level[1]. Cosmic-rays on ground level consist of mainly neutrons with wide energy range from MeV to GeV. A microscopic picture of the cosmic ray induced soft errors is the following. Energetic neutrons interact with materials used in the devices, and light charged particles and heavy ions can be generated via a nuclear reaction with a silicon nucleus. They can give rise to local charge burst in a micron volume, which results in upsets of the memory cell information quantum that are called “single-event upsets (SEUs)”. Therefore, quantitative estimation of the soft errors requires reliable nuclear reaction data for silicon in the high-energy range and modeling of charge transport in microelectronics devices.

So far, we have developed a database of cross sections for ^{28}Si at neutron energies between 20 MeV and 3 GeV, which is necessary for soft error simulation[2]. The database was successfully applied to calculations of neutron-induced SEU cross sections using the Burst Generation Rate (BGR) model [2,3] and a neutron-induced soft-error simulation code system for semiconductor memory devices[4].

In the future, the size of memory devices will be reduced, and it is expected that the influence of low energy neutrons on SEUs cannot be ignored because a critical charge causing the SEU becomes smaller[5]. In the present work, therefore, we have extended the database so as to include the cross sections below 20 MeV. Double-differential cross sections for all recoils in the $n+^{28}\text{Si}$ reaction are necessary for estimation of neutron-induced soft-errors. They were obtained using a kinematics calculation with the JENDL-3.3 library[6]. Finally, the cross section data were used to analyze some experimental data up to 160 MeV[7,8] by the BGR model calculation. In this report, we will discuss some results of the analysis, paying particular attention to SEUs for neutron energies below 20 MeV.

2. Development of database for $n+^{28}\text{Si}$ reaction

2.1 Outline

The JENDL-3.3 library[6] was used to obtain the double-differential cross sections (DDXs) for light charged particles (p and α) and all recoils ($^{24,25}\text{Mg}$, $^{27,28}\text{Al}$, and $^{27,28}\text{Si}$) in the $n+^{28}\text{Si}$ reaction at energies between 2 and 20 MeV. A method of processing the JENDL-3.3

library will be described in the next subsection. The data for energies between 20 to 150 MeV were taken from the LA150 library[9] in which the DDXs of all recoils are included. We have calculated the cross sections for energies above 150 MeV using the QMD[10] plus statistical decay model (GEM[11]) calculation.

2.2 Calculation of double-differential cross sections for recoils with JENDL-3.3

For neutron elastic and inelastic scattering, the emission energy and angle of the recoiled nucleus ^{28}Si can be easily obtained using the two-body kinematics [12], and the DDXs of ^{28}Si in the laboratory system are also converted from the data of differential neutron elastic and inelastic scattering cross sections in the JENDL-3.3 library. The same kinematics calculation was also applied to two heavy recoils, ^{28}Al and ^{25}Mg , produced by (n,p) and (n, α) reactions.

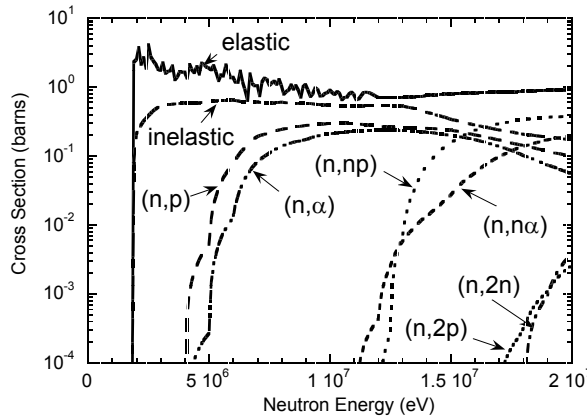
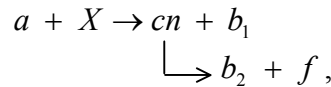


Fig.1 JENDL-3.3 cross sections for various reactions at neutron energies up to 20 MeV

As shown in **Fig.1**, two particle emission such as (n,np) and (n,n α) becomes dominant as the incident neutron energy increases and the influence on SEUs is expected to become crucial. However, it is not simple to obtain the DDXs of the recoils produced by the two-particle emission, because exclusive energy spectra for the second particle emission are not included in the JENDL-3.3. Note that the DDX spectra of the first neutron emission are included as MF=6, MT=16,22 and 28 in the JENDL-3.3. Hence, we assume that two-particle emission occurs via two-body sequential decay from the excited residual nucleus after the first particle emission:



where a and X are incident particle (neutron) and target nucleus (^{28}Si), and cn is the residual nucleus, ^{28}Si , after the first neutron (b_1) emission, and b_2 and f are the second emission particle and the recoil, respectively. The DDXs of the recoil nucleus, f , in the laboratory system are given by the following expression [13]:

$$\begin{aligned} \left(\frac{\partial^2 \sigma}{\partial \Omega_f \partial E_f} \right)^{\text{lab}} &= \int \left(\frac{\partial^2 \sigma}{\partial \Omega_{cn} \partial E_{cn}} \right) \frac{1}{\sigma_{dec}^{(t)}} \left(\frac{\partial^2 \sigma_{dec}}{\partial \Omega_f' \partial E_f'} \right) \left| \frac{\partial(\cos \theta_f', \phi_f', E_f')}{\partial(\cos \theta_f^{\text{lab}}, \phi_f^{\text{lab}}, E_f^{\text{lab}})} \right| d\Omega_{cn} dE_{cn} \\ &= \int \left(\frac{\partial^2 \sigma}{\partial \Omega_{cn} \partial E_{cn}} \right)^{\text{lab}} \frac{1}{\sigma_{dec}^{(t)}} \left(\frac{\partial^2 \sigma_{dec}}{\partial \Omega_f' \partial E_f'} \right) \left| \frac{\partial(\cos \theta_f', \phi_f', E_f')}{\partial(\cos \theta_f^{\text{lab}}, \phi_f^{\text{lab}}, E_f^{\text{lab}})} \right| d\Omega_{cn}^{\text{lab}} dE_{cn}^{\text{lab}}, \quad (1) \end{aligned}$$

where $(\partial^2 \sigma / \partial \Omega_{cn} \partial E_{cn})^{lab}$ is calculated from the data of DDXs of the emitted particle, b_1 , using the two-body kinematics, and $(\partial^2 \sigma_{dec} / \partial \Omega'_f \partial E'_f)$ is the DDX of the final recoil, f , in the rest frame of the compound nucleus, cn , and $\sigma_{dec}^{(i)}$ is the integrated cross section over Ω'_f and E'_f . $(\partial^2 \sigma_{dec} / \partial \Omega'_f \partial E'_f)$ is calculated by assuming the evaporation model for emission of b_2 and its isotropic angular distribution. In the evaporation model calculation, empirical formulae given in ref.[14] were used for the inverse cross sections of proton, α , and neutron, and the level density formula based on the Fermi-gas model was employed with the level density parameter $a=A/8$, where A is the mass number.

The DDXs for light-charged particles (proton and α) are included in the JENDL-3.3 library. Finally, a database of all DDXs for protons, α and all recoils($^{24,25}\text{Mg}$, $^{27,28}\text{Al}$, and $^{27,28}\text{Si}$) emitted in the $n+^{28}\text{Si}$ reaction were prepared for energies between 2 and 20 MeV.

3. Modified Burst Generation Rate (BGR) model

The SEU rate is defined by

$$\text{SEU rate} = \int \sigma_{SEU}(E_n) \phi(E_n) dE_n, \quad (2)$$

where $\sigma_{SEU}(E_n)$ is the SEU cross section for the neutron energy, E_n , and $\phi(E_n)$ is the neutron flux. Using the BGR method[2,3], $\sigma_{SEU}(E_n)$ is given by

$$\sigma_{SEU}(E_n) = C \cdot V \cdot BGR(E_n, Q_c, d), \quad (3)$$

where C is the charge collection efficiency and V is the sensitive volume per bit. It should be noted that the product of C and V is treated as a normalization parameter to be determined by fitting measured data of $\sigma_{SEU}(E_n)$. The BGR is defined as the probability that a nuclear reaction produces charged particles and ions which deposit the kinetic energy more than E_c in a sensitive volume, and is given as a function of incident neutron energy, E_n and critical charge, Q_c which can be converted into E_c using the relation E_c (MeV) = 22.5 Q_c (pC).

Since the energy deposit of the charged particles and ions in a small volume depends on the linear energy transfer (LET), we introduce an ‘‘effective depth d ’’ as a parameter for BGR calculations. Thus,

$$\begin{aligned} BGR(E_n, Q_c, d) &= \sum_i BGR(E_n, Q_c, d, A_i, Z_i) \\ &= N_{Si} \sum_i \int \int_{E_{\min}^{(i)}(d)}^{E_{\max}^{(i)}(d)} \left(\frac{d^2 \sigma}{dE d\Omega} \right)^{(i)} d\Omega dE, \end{aligned} \quad (4)$$

where N_{Si} is the number density of silicon atoms, and the index i stands for the kind of reaction product with mass number A_i and atomic number Z_i . $(d^2 \sigma / dE d\Omega)^{(i)}$ is the double-differential production cross section of the reaction product i . By taking into account the LET, the upper and lower limits of the integration, $E_{\max}^{(i)}(d)$ and $E_{\min}^{(i)}(d)$, are estimated as the maximum and minimum energies of the reaction product i that deposits the energy above E_c within d . The SRIM code[15] is used for calculations of the LET. It should be noted that isotropic angular distribution is assumed for emission of the reaction products for simplicity.

4. Results and discussion

Figures 2 and 3 shows a comparison of the calculation with measured data [7,8] for SRAMs with 256Kb or 1Mb. The measured data are normalized to the data of Cypress. The

normalization constant $C \cdot V$ in Eq.(3) was determined so that the BGR function calculated with $Q_c=53$ fC and $d=1.0$ μm gives a best fit to the data of Cypress. The obtained result shows satisfactory agreement with the measured data over the whole neutron energy range.

The region below 20 MeV in Fig.2 is expanded in Fig.3. The calculated SEU cross-sections are decomposed into individual contribution from each recoil nucleus. The recoil, ^{25}Mg , produced by the (n,α) reaction shows the largest contribution at energies below 17 MeV. Also, the recoil, ^{24}Mg , produced by the $(n,n\alpha)$ reaction affects considerably the SEUs with increase in neutron energy. In Fig.4, the energy spectra of all recoils are plotted at an incident energy of 20 MeV in order to see why these Mg isotopes have significant contributions to SEUs. The critical charge $Q_c=53$ fC corresponds to the energy deposit $E_{\text{dep}}=1.2$ MeV. The minimum energy of the recoil that can provide this energy deposit within $d=1.0$ μm is about 1.8 MeV ($E_{\text{min}}^{(i)}(d)$ in Eq.(4)). The energy spectra of Mg isotopes are distributed over the range above 1.8 MeV and have relatively large cross sections as can be seen in Fig.4. This is a possible reason why the Mg isotopes contribute significantly to SEUs.

Also, we have investigated the kind of reaction products that influence largely the SEUs for energies between 20 MeV and 150 MeV. The result is presented as a fraction of each recoil element to total SEUs in Fig.5. It is shown that production of heavy ions such as Al and Mg plays a major role in the SEUs at energies above 40 MeV, because such ions have large LET. It is also found that the contribution from Si is reduced with decrease in neutron energy. This trend can be explained by the fact that the elastic and inelastic cross sections become small and their angular distributions become steeper as the neutron energy increases.

Finally, the incident energy range having the most effect on the SEU rate has been examined by assuming a neutron flux distribution on the ground level given by IBM group[1]. The BGR functions are plotted for three different critical charges, $Q_c = 4.4, 13.3$ and 30 fC in Fig.6. The effective depth d is assumed to be 0.35 μm in the calculation. The product of the BGR and the neutron flux corresponding to the integrand in the right-hand side of Eq.(2) are shown in Fig.7 to examine the neutron sensitivity. It is found that the sensitivity increases remarkably at neutron energies below 20 MeV as Q_c decreases. This indicates that the nuclear data below 20 MeV will become important for estimation of soft-error rates as the size of memory devices is reduced because the reduction of the size leads to that of Q_c .

5. Conclusion

The database of cross sections for the $n+^{28}\text{Si}$ reaction was developed in the energy range between 2 MeV and 3 GeV for evaluations of the soft-errors in semiconductor memory devices induced by cosmic-ray neutrons. The data were applied to calculations of SEU cross sections using the modified BGR model that takes into account the effective depth in the sensitive volume as a parameter. The calculated results reproduced well the energy dependence of the measured SEU cross-sections for energies up to 160 MeV. It was found that the reaction products that influence the SEUs mainly are the heavy ions such as Mg and Al having large LET, particularly, the Mg isotopes have significant contribution at energies below 20 MeV. The dependence of the neutron sensitivity on the critical charge Q_c was investigated over neutron energies up to 150 MeV, and it was found that the sensitivity increases remarkably at neutron energies below 20 MeV with decrease in Q_c .

Acknowledgements

The authors are grateful to Mr. Y. Kawakami and Dr. M. Hane for valuable discussions on SER simulation calculation.

References

- [1] J.F. Ziegler et al., IBM J. Res. Develop. **40**, No.1 (1996).
- [2] T. Ikeuchi et al., J. of Nucl. Sci. and Technol., Suppl. **2**, 1380 (2002).
- [3] J.F. Ziegler and W. Lanford, Science **206**, 776 (1979).
- [4] Y. Kawakami et al., NEC Research & Development, **43**(2), 146 (2002).
- [5] H. Ibe et al., Applied Physics, **70**, No.11, 1308 (2001) [in Japanese].
- [6] K. Shibata et al., J. of Nucl. Sci. and Technol. **39**, 1125 (2002).
- [7] K. Johansson et al., IEEE Trans. Nucl. Sci. **45**, 2519 (1998).
- [8] K. Johansson et al., *ibid.* **46**, 1427 (1999).
- [9] M.B. Chadwick et al., Nucl. Sci. Eng. **131**, 293 (1998).
- [10] K. Niita et al., JQMD code, JAERI-Data/Code 99-042 (1999).
- [11] S. Furihata, Nucl. Inst. Method in Phys. Res. B **171**, 251 (2000); S. Furihata and T. Nakamura, J. Nucl. Sci. and Technol. Suppl. **2**, 758 (2002).
- [12] G.G. Ohlsen, Nucl. Instr. Methods, **37**, 240 (1965).
- [13] M.D. Baker et al., Nucl. Sci. Eng. **96**, 39 (1987).
- [14] A. Chatterjee et al., Pramana **16**, 391 (1981).
- [15] J.F. Ziegler, SRIM code (1999).

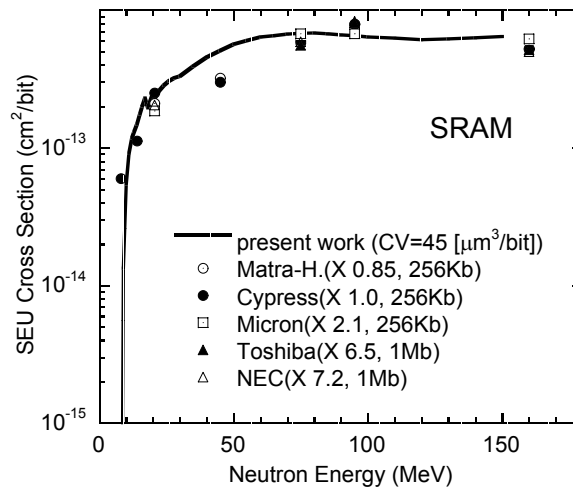


Fig.2 Comparison of the calculated SEU cross sections with the measured ones taken from Refs.[7,8]. The measured data are normalized to the data of Cypress.

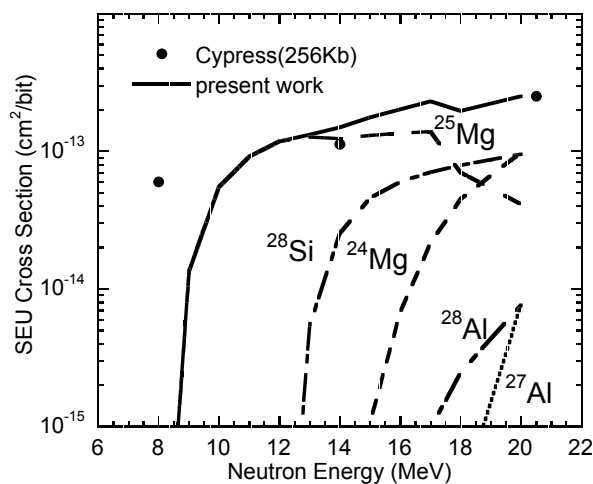


Fig.3 Same as in Fig.2, but the energy range below 20 MeV.

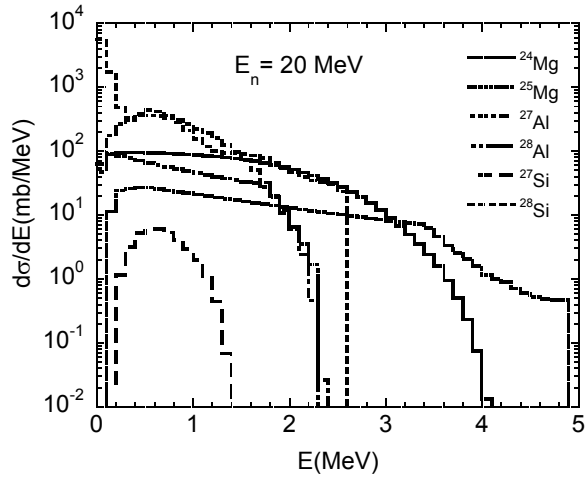


Fig.4 Energy spectra of all recoils for an incident energy of 20 MeV.

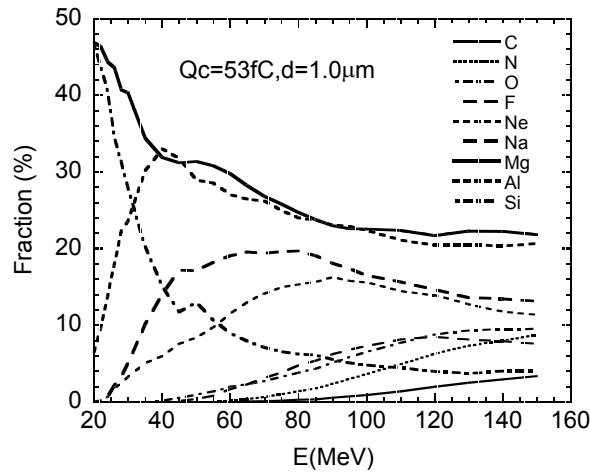


Fig.5 Fraction of each recoil element to total SEUs as a function of incident neutron energy.

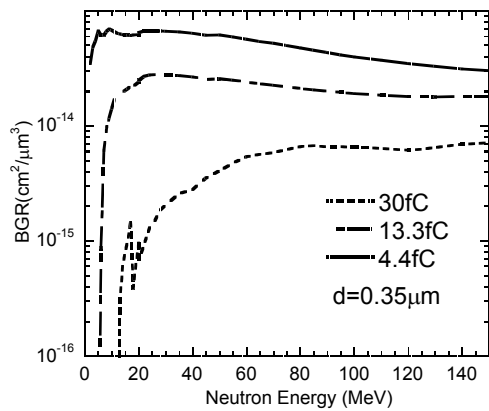


Fig.6 BGR functions for $Q_c=4.4, 13.3$ and 30 fC and effective depth $d=0.35 \mu\text{m}$.

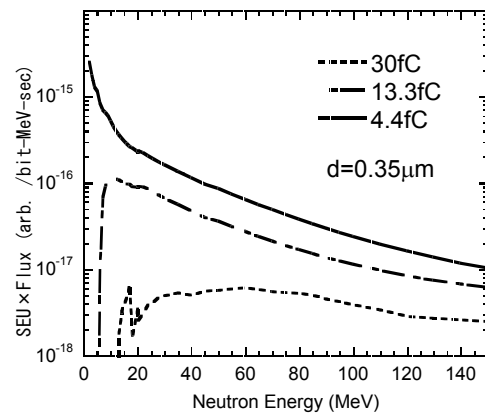


Fig.7 Sensitivity of the critical charge Q_c to SEUs for the cosmic-ray neutron flux given by IBM model[1].